Phenanthrene decomposition in soil washing effluents using UVB activation of hydrogen peroxide and peroxydisulfate

Yufang Tao, Olivier Monfort, Marcello Brigante, Hui Zhang, Gilles Mailhot

Journal Pre-proof

Phenanthrene decomposition in soil washing effluents using UVB activation of hydrogen peroxide and peroxydisulfate

Yufang Tao, Olivier Monfort, Marcello Brigante, Hui Zhang, Gilles Mailhot

PII: S0045-6535(20)32191-3

DOI: https://doi.org/10.1016/j.chemosphere.2020.127996

Reference: CHEM 127996

To appear in: *ECSN*

Received Date: 9 April 2020

Revised Date: 8 July 2020

Accepted Date: 10 August 2020

Please cite this article as: Tao, Y., Monfort, O., Brigante, M., Zhang, H., Mailhot, G., Phenanthrene decomposition in soil washing effluents using UVB activation of hydrogen peroxide and peroxydisulfate, *Chemosphere*, https://doi.org/10.1016/j.chemosphere.2020.127996.

Abstract

In this work, the decomposition of phenanthrene (PHE) in mimic and real soil washing (SW) effluents was investigated using UVB light assisted activation of hydrogen peroxide (H_2O_2) and peroxydisulfate (PDS) oxidation processes. The impact of oxidant concentration, initial pH, and coexisting inorganic anions (Cl^-, HCO_3^- and NO_3^-) on PHE removal was evaluated. PHE degradation efficiency under UVB irradiation followed the order of UVB/PDS > UVB/H_2O_2 > UVB. The increase of PHE decomposition efficiency was observed with increasing oxidant dose in the range of 2−30 mM upon the two processes. It was found Cl^- played different roles in the two activation systems depending on the solution pH and Cl^- concentration. The influence of HCO_3^- on PHE elimination was negligible in the UVB/PDS process, while an inhibitory effect was observed in the UVB/H_2O_2 system. Nitrate inhibited the PHE decay in both UVB/H_2O_2 and UVB/PDS processes at the investigated pH 3.3, 7.1 and 8.6. Finally, the application of the two activation processes to the treatment of real SW effluents indicated that up to 85.0% of PHE degradation could be reached under 6 h UVB irradiation with PDS, indicating UVB/PDS process is a promising alternative for SW effluent treatment.

Keywords: Soil washing effluent; Phenanthrene; Peroxydisulfate; Hydrogen peroxide; Photodegradation.

Phenanthrene decomposition in soil washing effluents using UVB activation of hydrogen peroxide and peroxydisulfate

Yufang Tao[a,b], Olivier Monfort[b], Marcello Brigante[b], Hui Zhang[a*], Gilles Mailhot[b*]

[a] Department of Environmental Science and Engineering, Wuhan University, 430079, China

[b] Université Clermont Auvergne, CNRS, SIGMA Clermont, Institut de Chimie de Clermont-Ferrand, F-63000 Clermont–Ferrand, France

Corresponding authors: eeng@whu.edu.cn (H. Zhang);

gilles.mailhot@uca.fr (G. Mailhot).

Abstract

In this work, the decomposition of phenanthrene (PHE) in mimic and real soil washing (SW) effluents was investigated using UVB light assisted activation of hydrogen peroxide (H_2O_2) and peroxydisulfate (PDS) oxidation processes. The impact of oxidant concentration, initial pH, and coexisting inorganic anions (Cl^-, HCO_3^- and NO_3^-) on PHE removal was evaluated. PHE degradation efficiency under UVB irradiation followed the order of UVB/PDS > UVB/H_2O_2 > UVB. The increase of PHE decomposition efficiency was observed with increasing oxidant dose in the range of 2−30 mM upon the two processes. It was found Cl^- played different roles in the two activation systems depending on the solution pH and Cl^- concentration. The influence of HCO_3^- on PHE elimination was negligible in the UVB/PDS process, while an inhibitory effect was observed in the UVB/H_2O_2 system. Nitrate inhibited the PHE decay in both UVB/H_2O_2 and UVB/PDS processes at the investigated pH 3.3, 7.1 and 8.6. Finally, the application of the two activation processes to the treatment of real SW effluents indicated that up to 85.0% of PHE degradation could be reached

under 6 h UVB irradiation with PDS, indicating UVB/PDS process is a promising alternative for SW effluent treatment.

Keywords: Soil washing effluent; Phenanthrene; Peroxydisulfate; Hydrogen peroxide; Photodegradation.

1. Introduction

Contamination of soils by toxic pollutants, especially by the recalcitrant hydrophobic organic compounds (HOCs) is a matter of significant public, scientific and regulatory concern. Polycyclic aromatic hydrocarbons (PAHs), as a class of HOCs, are ubiquitous in the soil environment due to their low solubility in water and long-term persistence in soils (Manoli and Samara 1999; Shin et al., 2006; Trellu et al., 2016). Phenanthrene (PHE), containing three benzene rings, is one of the most widely detected PAHs in the contaminated sites (Bezza and Chirwa 2017; Gou et al., 2019; Li et al., 2019; Petrová et al., 2017), especially those located in manufactured gas plants and coal tar refinery (Li et al., 2019; Reddy et al., 2006; Yeom et al., 1995). Therefore, it is urgent and essential to develop effective remediation strategies to restore PAHs contaminated soil.

Surfactant-enhanced *ex*-situ soil washing (SW) has been proposed as a promising technology for elimination of PHE from contaminated soils due to its high extraction efficiency and low remediation cost (Kuhlman and Greenfield 1999; Ortega et al., 2008). Among various surfactants, Tween 80 (TW80) was the most commonly used non-ionic surfactant for washing PHE and other PAHs from soil due to its high solubilization capacity, low cost and low toxicity (Cheng et al., 2017; Lamichhane et al., 2017). Nevertheless, the SW process generates a large amount of effluent containing soil pollutant and surfactant, which should be further treated with

appropriate methods for the complete elimination of soil pollutant (Mousset et al., 2014; Trellu et al., 2017).

In the past few decades, advanced oxidation processes (AOPs) have been developed and widely applied as alternative technologies for the degradation of recalcitrant pollutants in waters and soils (Liu et al., 2016; Mousset et al., 2014; Wan et al., 2018; Wu et al., 2015). This is mainly attributed to the formation of reactive species with high standard redox potential such as hydroxyl radical ($HO^{\bullet}$, E^0 = 1.8-2.7 V) or sulfate radical ($SO_4^{\bullet-}$, E^0 = 2.5-3.1 V) (Buxton et al., 1988; Neta et al., 1988). As efficient and environmental friendly techniques, $HO^{\bullet}$ or $SO_4^{\bullet-}$ based AOPs have been extensively investigated for the treatment of contaminants in water under UV irradiation (UVA, UVB and UVC) (Huang et al., 2018; Minella et al., 2019; Mosteo et al., 2020; Xiao et al., 2016; Xu et al., 2016; Yang et al., 2016; Zhang et al., 2015; Zhou et al., 2017b). Compared with UVA and UVC, UVB based oxidation has great potential due to: *i*) possible use of LED *ii*) considerably less energy requirement than UVC (Beck et al., 2017) and *iii*) higher efficiency for contaminant degradation than UVA (Joseph et al., 2016). After reviewing the literature, it is found that the investigation on HOCs decomposition by UVB-based oxidation is pretty limited and no studies for systematic comparison of SW effluent treatment by UVB activation of PDS and H_2O_2 are reported before.

The presence of inorganic anions has been reported to exert strong impacts on the oxidative degradation of contaminants (Bennedsen et al., 2012; Liu et al., 2016; Yang et al., 2014). However, the effect of these anions on the photo-degradation of PHE in the SW effluent has not been investigated before. In this study, for the first time, UVB irradiation was used to activate H_2O_2 and PDS for PHE decomposition in a surfactant co-existing SW effluent. The aims of this work were: (1) to investigate the PHE

decomposition efficiency in the present of TW80 by direct UVB radiation, UVB/H_2O_2, and UVB/PDS processes; (2) to evaluate the impact of operating factors including the oxidant dosage, the initial pH and the coexisting anions on PHE treatment efficiency; (3) to assess the performance of UVB, UVB/H_2O_2 and UVB/PDS systems on PHE oxidation in the real SW solutions.

2. Materials and methods

2.1 Chemicals

TW80, phenanthrene (PHE), sodium persulfate ($Na_2S_2O_8$, ≥ 99.0%), sodium chorine (NaCl, ≥ 99.5%), sodium bicarbonate ($NaHCO_3$, ≥ 99.7%) and sodium nitrate ($NaNO_3$, ≥ 99.0%) were purchased from Sigma-Aldrich. Hydrogen peroxide (H_2O_2, 30%) was obtained from Fluka, France. Perchloric acid ($HClO_4$) and sodium hydroxide (NaOH) were applied for adjusting the initial pH of the solutions. Millipore Ultra-Pure System purified water (18.2 MΩ cm) was used to prepare solutions. All the chemical reagents were of analytical grade and employed without further purification.

2.2 Preparation of the mimic and real SW solutions

One liter of mimic SW solution was prepared as previously reported (Tao et al., 2019). Briefly, 10 mg of PHE was added to 1 L aqueous solution containing 0.5 g L^{-1} TW80. The mixed solution was vigorously stirred for one week to obtain complete PHE dissolution before irradiation experiments.

Natural soil samples were obtained from Wuhan of Hubei Province (soil 1), Chuzhou of Anhui Province (soil 2) and Huaian of Jiangsu Province (soil 3), respectively. The collected soils were air dried and ground to obtain particles less than 2 mm before use. The PHE contaminated soil samples were prepared according to the literature (Yang et al., 2006). Briefly, the three PHE free soils were spiked with PHE dissolved in acetone

solutions and vigorously stirred for 30 minutes to obtain homogeneous distribution of PHE in the soil. The spiked soil samples were placed in three hoods for 5 days at room temperature to evaporate the solvent. The final PHE concentrations of each spiked soil were 4000 mg kg^{-1}.

To obtain the real SW solutions, 3 grams of each contaminated soil were separately weighed into 150 mL conical flasks with stoppers and 60 mL TW80 solutions (10 g L^{-1}) were added. The flasks were then placed into a constant temperature shaker for 24h with a speed of 200 rpm at 25 ^{o}C. Then, the mixtures were centrifuged at 8000 rpm for 15 min and the supernatants were filtered with 0.22 μm PTFE filters before analysis and the sequent irradiation experiments.

2.3 Irradiation experiments

Irradiations experiments were carried out in a cylindrical Pyrex reactor (100 mL) which was placed into a rectangular glass jacket vessel with cooling water flowing between interlayers ensuring a constant temperature of 20 ± 2 ^{o}C through a thermostat-controlled cooling system. Four UVB tubes (G15T8E, Japan) were fixed on the top of the photo-reactor as the light resource, and the distance between photoreactor and the lamps was around 24 cm. The schematic diagram of experimental set-up is shown in Figure S1.

The polychromatic UVB irradiation energy was recorded by an optical fiber with a charge coupled device spectrophotometer (Ocean Optics USD 2000 + UV–vis). The total irradiance reaching the solution was then estimated to be 1393 μW cm^{-2} in the UVB range (between 270 and 400 nm). The absorption spectra of PDS, H_2O_2 and PHE solution in TW80 were recorded with a UV-visible spectrophotometer Cary 300. Emission spectrum of adopted UVB lamps reaching the solution was recorded using a calibrated CCD camera (Huang et al., 2018) as presented in Figure S2.

During the irradiation, the SW solution was continuously magnetically stirred at a fixed speed with a magnetic stirrer. At fixed interval times, 1 mL of sample was withdrawn and analyzed by a high performance liquid chromatography (HPLC, Alliance) equipped with a Waters 2998 photodiode array detector. The flow rate was 1 mL min^{-1} and an isocratic elution with water and acetonitrile (15/85, v/v) was used. The column was a Nucleodur 100-5 C18 of 150 mm × 4.6 mm, with particle size of 5 μm.

The pseudo-first order rate constant of PHE decomposition (k_1) was determined from Eq. (1):

$$[PHE]/[PHE]_0 = \exp(-k_1 t) \quad (1)$$

where $[PHE]_0$ and [PHE] were the PHE initial concentration and PHE concentration at time *t*, respectively.

Inorganic components of three real SW effluents were determined by ion chromatography. For anions, a Dionex DX320 system equipped with an IonPac AS11 column and a KOH elution in gradient mode were used. For cations, a Dionex ICS-1500 system equipped an Ion-Pac CS16 column and a metasulfonic acid (MSA) eluent were employed (Marion et al., 2018).

TW80 concentration after soil washing process was quantified by a spectrophotometric method using cobalt ammonium thiocyanate as the chromogenic agent (Crabb and Persinger 1964).

3. Results and discussion

3.1 Comparison of UVB activation of H_2O_2 and PDS

In Figure 1, the decomposition of PHE (10 mg L^{-1} corresponding to ~56 μM in 0.5 g L^{-1} TW80 solution) is reported. Under direct photolysis (UVB alone), about 23.0%

of PHE decay was observed after 3 h irradiation with a first order rate constant (k_1) of 1.5×10^{-3} min^{-1}, which is equivalent to a half-life of 7.8 h (Table S4). When the oxidant (H_2O_2 or PDS) was applied to the irradiation system, $HO^{\bullet}$ and $SO_4^{\bullet-}$ were generated through photo-dissociation of H_2O_2 and PDS under UVB irradiation (Eqs. 2 and 3) (Mark et al., 1990; Yu and Barker 2003).

$$S_2O_8^{2-} + h\upsilon \rightarrow 2SO_4^{\bullet-} \quad (2)$$

$$H_2O_2 + h\upsilon \rightarrow 2HO^{\bullet} \quad (3)$$

The evolution of HPLC chromatograms during UVB/H_2O_2 and UVB/PDS processes is presented in Figure S3, and PHE removal reached up to 34.0% and 72.0%, respectively. The pseudo-first order rate constants were 2.3×10^{-3} min^{-1} with H_2O_2 and 7.1×10^{-3} min^{-1} with PDS. The correspondent half-lives of PHE were calculated to be 5.0 h and 1.6 h in the UVB/H_2O_2 and UVB/PDS systems, respectively (Table S4). The different performance between UVB/H_2O_2 and UVB/PDS systems could be ascribed to the following aspects. Firstly, the photo-dissociation quantum yield of PDS is higher than that for H_2O_2. In fact, near the maximum emission wavelength of UVB (313 nm in Figure S2), the reported $SO_4^{\bullet-}$ formation quantum yield from PDS photolysis ($\Phi_{SO_4^{\bullet-}}$) is 1.1 ± 0.2 (Herrmann 2007), which is higher than the quantum yield for $HO^{\bullet}$ generation from H_2O_2, i.e., 0.98 ± 0.2 (Zellner et al., 1990) or 0.8 ± 0.2 (Yu and Barker 2003) at the wavelength of 308 nm. Secondly, the selectivity of $SO_4^{\bullet-}$ towards PHE is superior to that of $HO^{\bullet}$ (Tao et al., 2019). To verify this point, the selectivity coefficient ζ_{PHE} is defined as Eq. (4) based on the reactions of radicals with PHE, TW80 (Eqs. 5-8) and other species in the system (see Text S1).

$$\zeta_{PHE} = \frac{k_{X^{\bullet},PHE}[PHE]_0}{k_{X^{\bullet},PHE}[PHE]_0 + k_{X^{\bullet},S}[S]_0} \quad (4)$$

where $k_{X^{\bullet},PHE}$ and $k_{X^{\bullet},S}$ are the second order rate constants of radicals with PHE and other components S (PHE, TW80, oxidant, etc.) in the system, respectively. $[PHE]_0$ and $[S]_0$ are their initial concentrations.

$$PHE + HO^{\bullet} \rightarrow \text{products} \qquad k_{HO^{\bullet},PHE} = 6.1 \times 10^9\ M^{-1}\ s^{-1} \qquad (5)$$

$$PHE + SO_4^{\bullet-} \rightarrow \text{products} \qquad k_{SO_4^{\bullet-},PHE} = 4.3 \times 10^9\ M^{-1}\ s^{-1} \qquad (6)$$

$$TW80 + HO^{\bullet} \rightarrow \text{products} \qquad k_{HO^{\bullet},TW80} = 9.9 \times 10^9\ M^{-1}\ s^{-1} \qquad (7)$$

$$TW80 + SO_4^{\bullet-} \rightarrow \text{products} \qquad k_{SO_4^{\bullet-},TW80} = 4.6 \times 10^9\ M^{-1}\ s^{-1} \qquad (8)$$

In the UVB/H_2O_2 system, $HO^{\bullet}$ is the main generated radical, and ζ_{PHE} was calculated to be around 8.1%, while the selectivity coefficient was about 12.1 % in the UVB/PDS system with $SO_4^{\bullet-}$ as the major radical. This means the selectivity coefficient ζ_{PHE} for $SO_4^{\bullet-}$ towards PHE (12.1%) is about 1.5 times higher than that of $HO^{\bullet}$ (8.1%). The result confirms $SO_4^{\bullet-}$ was more selective than $HO^{\bullet}$ to the oxidation of PHE in the presence of TW80 (Tao et al., 2019). Lastly, the rate constant of H_2O_2 and $HO^{\bullet}$ is around 43 times higher than that of PDS and $SO_4^{\bullet-}$ ($k_{HO^{\bullet},H_2O_2} = 2.7 \times 10^7\ M^{-1}\ s^{-1}$, $k_{SO_4^{\bullet-},S_2O_8^{2-}} = 6.3 \times 10^5\ M^{-1}\ s^{-1}$), indicating $HO^{\bullet}$ would be more prone to be quenched by H_2O_2 than $SO_4^{\bullet-}$ scavenged by PDS (Eqs. 9 and 10).

$$HO^{\bullet} + H_2O_2 \rightarrow H_2O + HO_2^{\bullet} \qquad k_{HO^{\bullet},H_2O_2} = 2.7 \times 10^7\ M^{-1}\ s^{-1} \qquad (9)$$

$$SO_4^{\bullet-} + S_2O_8^{2-} \rightarrow SO_4^{2-} + S_2O_8^{\bullet-} \qquad k_{SO_4^{\bullet-},S_2O_8^{2-}} = 6.3 \times 10^5\ M^{-1}\ s^{-1} \qquad (10)$$

3.2 Effect of oxidant concentration

Effects of initial concentration of H_2O_2 or PDS on PHE degradation were evaluated as reported in Figure 2. In the UVB/H_2O_2 process, it can be seen from Figure 2A that PHE decomposition after 3 hours reached around 28.0% with 2 mM H_2O_2 and 51.0% with 30 mM H_2O_2, and the corresponding PHE oxidation rate constant increased around 1.95 folds from 2.0×10^{-3} to 3.9×10^{-3} min^{-1}. In the UVB/PDS process as

illustrated in Figure 2B, with 2 mM of PDS, the PHE decomposition efficiency reached around 61.0% and rate constant was 5.1×10^{-3} min^{-1}. With further addition of PDS to 30 mM, the PHE elimination efficiency was around 83.0% and k_1 increased around 1.90 folds to 9.7×10^{-3} min^{-1}. In comparison with the effect of oxidant type, the results indicated that the decomposition efficiency of PHE followed the order of PDS > H_2O_2 at the same oxidant dosage.

Some researchers reported that the decomposition rate of contaminant increased linearly with the oxidant dosage (Deng et al., 2013; Tan et al., 2013; Xu et al., 2016), while others found that the removal rate would drop when the oxidant concentration exceeds its threshold level (Olmez-Hanci and Arslan-Alaton 2013; Yang et al., 2010; Zhou et al., 2017a). In our case, PHE removal increased almost linearly with increasing H_2O_2 concentration from 2 to 30 mM, probably because more $HO^{\bullet}$ radcials were formed for PHE decomposition with higher H_2O_2 concentration and the maximum dosage (30 mM) was still below its threshold level. In the UVB/PDS system, PHE removal efficiency also increased with the increasement of PDS. However, insignificant improvement of PHE decomposition was observed at PDS concentration higher than 10 mM, which possibly because the PDS concentration was beyond the threshold and quenching effect of $SO_4^{\bullet -}$ radicals via Eq. (10) (Herrmann et al., 1995) became pronounced.

3.3 Effect of initial pH

The influence of initial pH on the photo-degradation of PHE by the UVB/H_2O_2 and UVB/PDS processes is given in Figure 3. In the UVB/H_2O_2 system, a slight difference (less than 10.0%) was obtained from pH 3.3 to pH 10.1, though the maximum PHE decomposition extent of 40.0% and a first order rate constant of 2.8×10^{-3} min^{-1} were

observed at pH 4.5 (Figure 3A). In the UVB/PDS system, pH had insignificant effect on PHE decay, and the difference of PHE photo-degradation efficiency was less than 5.0% with pH value ranging from acidic to basic (Figure 3B). The little difference of PHE degradation with pH is probably due to the chemical stability of PHE with pH ranging from 3.3 to 10.1 and also the photolysis of H_2O_2 or PDS is not pH dependent. Moreover, although the PHE degradation was performed in a quite wide initial pH range (from 3.3 to 10.1), the pH varied from 3.4 to 6.6 after UVB/H_2O_2 process, or from 3.3 to 3.8 after UVB/PDS process as indicated in Table S5. The difference of final pH (3.3~3.8) in the UVB/PDS system is less than that (3.4~6.6) in the UVB/H_2O_2 system. It is probably due to the higher degradation efficiency of PHE and more production of acidic intermediates in the UVB/PDS system than in the UVB/H_2O_2 system.

3.4 Effect of inorganic anions

Inorganic species (such as carbonate, chloride and nitrate) are widely found in the soil due to many factors: (i) the parent soil substrate, (ii) depositions through fertilization, and (iii) other human activities such as irrigation (Du et al., 2013; Wang et al., 2019). These anions are generally considered to be freely mobile in soils and can be released into groundwater *via* rainfall (Bastviken et al., 2006; Lu et al., 2019). Therefore, inorganic species (Cl^-, HCO_3^- and NO_3^-) are inevitably dissolved in the SW effluent and they may exert impact on the PHE decomposition by UVB/H_2O_2 and UVB/PDS processes.

3.4.1 Chloride

The PHE elimination as a function of Cl^- dosage at pH 3.3 of the two AOP systems is presented in Figure 4. The results clearly revealed that the presence of Cl^- had adverse effect on the two AOPs. In the UVB/H_2O_2 process as shown in Figure 4A, the effect of 2 and 10 mM Cl^- on PHE oxidation was insignificant, while PHE decay was

inhibited by around 10.0% with addition of 50 mM Cl^-. In the UVB/PDS process as depicted in Figure 4B, PHE oxidation gradually increased by 9.0% when Cl^- concentration ranging from 0 to 10 mM and no further improvement of PHE removal can be achieved with 50 mM Cl^-. At pH 7.1, the influence of Cl^- from 2 to 50 mM on PHE removal is negligible in the UVB/H_2O_2 system (Figure S4A), while PHE removal increased by 15.0% with Cl^- dose varying from 0 to 50 mM in the UVB/PDS process (Figure S4B). At alkaline pH 8.6, Cl^- exerted negative effect on PHE oxidation and larger inhibition was observed with higher Cl^- concentration in the UVB/H_2O_2 system and PHE decomposition decreased by 17.0% in the presence of 50 mM Cl^- (Figure S4C). Under the same pH condition, the effect of 2 mM Cl^- on PHE removal was insignificant and PHE removal was slightly promoted by around 6.0% with 10 and 50 mM Cl^- in the UVB/PDS system (Figure S4D).

Various conflicting results were reported in the different UV based AOPs with the presence of Cl^- as indicated in Table S1. Usually, Cl^- can react with $HO^\bullet$ and $SO_4^{\bullet-}$ to yield secondary active chlorine radical species such as $ClOH^{\bullet-}$, $Cl^\bullet$, and $Cl_2^{\bullet-}$ through a series of intricate chain reactions (Eqs. 11, 13-15) (Grigor'ev et al., 1987; Jayson et al., 1973; Neta et al., 1988).

$$HO^\bullet + Cl^- \rightarrow ClOH^{\bullet-} \qquad k_{HO^\bullet,Cl^-} = 4.3 \times 10^9\ M^{-1}s^{-1} \qquad (11)$$

$$ClOH^{\bullet-} \rightarrow Cl^- + HO^\bullet \qquad k_{ClOH^{\bullet-},ClOH^{\bullet-}} = 6.1 \times 10^9\ M^{-1}\ s^{-1} \qquad (12)$$

$$ClOH^{\bullet-} + H^+ \rightarrow Cl^\bullet + H_2O \qquad k_{ClOH^{\bullet-},H^+} = 2.1 \times 10^{10}\ M^{-1}\ s^{-1} \qquad (13)$$

$$Cl^\bullet + Cl^- \rightarrow Cl_2^{\bullet-} \qquad k_{Cl^\bullet,Cl^-} = 2.1 \times 10^{10}\ M^{-1}\ s^{-1} \qquad (14)$$

$$ClOH^{\bullet-} + Cl^- \rightarrow Cl_2^{\bullet-} + HO^- \qquad k_{ClOH^{\bullet-},Cl^-} = 1.0 \times 10^4\ M^{-1}\ s^{-1} \qquad (15)$$

$$Cl_2^{\bullet-} + PHE \rightarrow \text{byproducts} \qquad k_{Cl_2^{\bullet-},PHE} = 4.6 \times 10^8\ M^{-1}\ s^{-1} \qquad (16)$$

The negligible effect of low Cl^- concentration (2–10 mM) on PHE removal in the UVB/H_2O_2 system was mainly due to the reaction of Eq. (12). The negative effect of

50 mM Cl^- on PHE oxidation observed can be ascribed to the consumption of H_2O_2 by $Cl^{\bullet}$ and $Cl_2^{\bullet-}$ (Eqs.17 and 18) (Hasegawa and Neta 1978; Kläning and Wolff 1985). These reactions reduced the amount of available $HO^{\bullet}$ and $Cl_2^{\bullet-}$ radicals reacting with PHE (Eqs.5 and 16) (Tao et al., 2019), leading to the lower PHE elimination. Moreover, the finding of inhibition of PHE at pH 8.6 could be explained by the reduction of $Cl_2^{\bullet-}$ triggered by Eqs. (19) and also the higher consumption of H_2O_2 via Eqs. (17) and (18) at alkaline pH, which restrained active species reacting with PHE and consequently retarded PHE oxidation.

$$Cl^{\bullet} + H_2O_2 \rightarrow H^+ + Cl^- + HO_2^{\bullet} \qquad k_{Cl^{\bullet},H_2O_2} = 2.0 \times 10^9\ M^{-1}\ s^{-1} \qquad (17)$$

$$Cl_2^{\bullet-} + H_2O_2 \rightarrow HO_2^{\bullet} + H^+ + 2Cl^- \qquad k_{Cl_2^{\bullet-},H_2O_2} = 1.4 \times 10^5\ M^{-1}\ s^{-1} \qquad (18)$$

$$Cl_2^{\bullet-} + HO^- \rightarrow ClOH^{\bullet-} + Cl^- \qquad k_{Cl_2^{\bullet-},HO^-} = 4.5 \times 10^7\ M^{-1}\ s^{-1} \qquad (19)$$

In the UVB/PDS system, the weak enhancement of PHE decay was attributed to the production of $Cl_2^{\bullet-}$ radicals through a series of chain reactions (Eqs.14 and 20). According to our previous study (Tao et al., 2019), $Cl_2^{\bullet-}$ was more selective towards PHE than $SO_4^{\bullet-}$ in the presence of TW80 (Eqs. 16 and 21), therefore PHE elimination could be promoted.

$$SO_4^{\bullet-} + Cl^- \rightarrow SO_4^{2-} + Cl^{\bullet} \qquad k_{SO_4^{\bullet-},Cl^-} = 4.7 \times 10^8\ M^{-1}\ s^{-1} \qquad (20)$$

$$Cl_2^{\bullet-} + TW80 \rightarrow \text{byproducts} \qquad k_{Cl_2^{\bullet-},TW80} = 7.1 \times 10^6\ M^{-1}\ s^{-1} \qquad (21)$$

3.4.2 Bicarbonate

Figure 5 depicts the elimination efficiency of PHE in the presence of various concentrations of bicarbonate (HCO_3^-) in the UVB/H_2O_2 and UVB/PDS processes at initial pH of around 8.6. As presented in Figure 5A, the oxidation of PHE was obviously inhibited with the addition of HCO_3^-, which is in accordance with most reports investigated in aqueous phase in the absence of surfactant (Table S2). With the addition of 50 mM bicarbonate, the PHE removal efficiency decreased by almost

294 one-half in comparison with 33.0% removal in the absence of bicarbonate. HCO_3^-
295 could react with $HO^\bullet$ to generate carbonate radicals ($CO_3^{\bullet-}$) via Eq. (22). However, the
296 generated $CO_3^{\bullet-}$ are considered to be a weaker oxidant and the reactions with most
297 organic pollutants are insignificant (Crittenden et al., 1999; Zuo et al., 1999). As a
298 consequence, available $HO^\bullet$ was reduced and PHE decomposition was depressed.

299 $$HCO_3^- + HO^\bullet \rightarrow H_2O + CO_3^{\bullet-} \qquad k_{HO^\bullet,HCO_3^-} = 8.5 \times 10^6\ M^{-1}\ s^{-1} \qquad (22)$$

300 The effect of bicarbonate in the UVB/PDS system is illustrated in Figure 5B.
301 Insignificant effect of HCO_3^- was observed, which may be ascribed to the negligible
302 scavenging effect of $SO_4^{\bullet-}$ by HCO_3^- (Eq. 23) since the rate constant between $SO_4^{\bullet-}$
303 and HCO_3^- is around 3 orders of magnitudes smaller than that between PHE and
304 $SO_4^{\bullet-}$. In the meanwhile, the little influence of HCO_3^- on the performance of
305 UVB/PDS system was ascribed to the unpronounced variation of selectivity
306 coefficient (12.1% ~ 11.3%) with the HCO_3^- concentration ranging from 0 ~ 50 mM.

307 $$HCO_3^- + SO_4^{\bullet-} \rightarrow SO_4^{2-} + CO_3^{\bullet-} + H^+ \quad k_{SO_4^{\bullet-},HCO_3^-} = 2.8 \times 10^6\ M^{-1}\cdot s^{-1} \qquad (23)$$

308 **3.4.3 Nitrate**

309 The influence of NO_3^- with different doses and pH conditions on the
310 decomposition of PHE in the UVB/PDS and UVB/H_2O_2 systems were studied. NO_3^-
311 led to a strong inhibitory effect on the two AOPs, which is in agreement with other
312 reports as summarized in Table S3. At pH 3.3, with the concentration of NO_3^- ranging
313 from 0 to 50 mM, the PHE decomposition efficacy decreased from 34.5% to 19.0% in
314 the UVB/H_2O_2 system (Figure 6A), while it dropped from 73.0% to 42.0% in the
315 UVB/PDS system (Figure 6B).

316 The stronger inhibition of NO_3^- on PHE decomposition can be explained by the
317 screen effect of light due to the photoreactivity of NO_3^- (Eqs. 24 and 25) (Keen et al.,
318 2012) and its secondary substance (i.e. NO_2^-), leading to competition with H_2O_2 and

PDS for UVB radiation. It is reported that both NO_3^- and NO_2^- have absorption in the range of UVB light (around 260 – 330 nm) (Mack and Bolton 1999). This is supported by the strong decrease of the direct photolysis of PHE under UVB irradiation in presence of 5 mM NO_3^-. In the UVB alone, PHE removal was 23.0% while it dropped to only 7.0% with the addition of 5 mM NO_3^-. The production of $HO^\bullet$ from the NO_3^- and NO_2^- photolysis (Eqs. 26-28) (Keen et al., 2012; Lyon et al., 2012; Sörensen and Frimmel 1997) probably did not compensate the negative screen effect. On the other hand, NO_3^- and NO_2^- had quenching effect for both $SO_4^{\bullet-}$ and $HO^\bullet$ via Eqs. (29)-(31), which could also restrain PHE degradation.

$$NO_3^- + h\upsilon \rightarrow NO_2^\bullet + O^{\bullet-} \quad (24)$$

$$NO_3^- + h\upsilon \rightarrow NO_2^- + 1/2O_2 \quad (25)$$

$$NO_3^- + H^+ + h\upsilon \rightarrow HO^\bullet + NO_2^\bullet \quad (26)$$

$$NO_2^- + H^+ + h\upsilon \rightarrow HO^\bullet + NO^\bullet \quad (27)$$

$$O^{\bullet-} + H^+ \leftrightharpoons HO^\bullet \qquad pKa = 11.9 \quad (28)$$

$$NO_2^- + HO^\bullet \rightarrow NO_2^\bullet + HO^- \qquad k_{HO^\bullet,NO_2^-} = 1.0 \times 10^{10}\ M^{-1}\cdot s^{-1} \quad (29)$$

$$NO_3^- + SO_4^{\bullet-} \rightarrow NO_3^\bullet + SO_4^{2-} \qquad k_{SO_4^{\bullet-},NO_3^-} = 5.0 \times 10^{4}\ M^{-1}\cdot s^{-1} \quad (30)$$

$$NO_2^- + SO_4^{\bullet-} \rightarrow NO_2^\bullet + SO_4^{2-} \qquad k_{SO_4^{\bullet-},NO_2^-} = 8.8 \times 10^{8}\ M^{-1}\cdot s^{-1} \quad (31)$$

The influence of 5 mM NO_3^- on PHE degradation at different initial pH was also investigated in the two AOPs. As displayed in Figure S5, in comparison with the absence of NO_3^-, the decrease of PHE removal at pH 3.3, 7.1 and 8.6 was respectively 5.0%, 14.5%, 13.6% in the UVB/H_2O_2 system, while it was respectively 10.7%, 10.3% and 14.3% in the UVB/PDS system.

3.5 Treatment of real SW effluent by the UVB/H_2O_2 and UVB/PDS systems

The treatment of real effluents after washing three types of soils spiked with PHE was further carried out to evaluate the feasibility of UVB/H_2O_2 and UVB/PDS systems. The various ions and constituents in the soils are listed in Table S6, and the results of SW effluent treatment are displayed in Figure 7. As can be seen, UVB/PDS system was more effective for PHE decomposition than UVB/H_2O_2 and UVB alone for the three SW samples, corroborating our former results with mimic SW samples. Direct PHE photolysis in the UVB system was less than 10.0% for all the three SW effluents. The lower efficiency compared with synthetic SW samples (around 23.0%) could be ascribed to the screening effect of light due to the diverse mixture of substances in the solution. For UVB/H_2O_2 or UVB/PDS process the efficiencies of PHE degradation in the SW effluents from soil 1 and 2 were comparable with those in the synthetic SW effluents, while for soil 3, the PHE removal efficiency was lower in both UVB/H_2O_2 and UVB/PDS systems. In fact, with H_2O_2, PHE degradation efficiencies after 6 h irradiation were 47.5%, 51.6% and 33.5% in soil 1, 2 and 3 respectively. With PDS the removal of PHE achieved around 85.0% for soil 1 and 2 and 78.0% for soil 3.

The results of PHE degradation with the three real SW effluents using the two AOPs validated our previous observations on the mimic SW solutions and the effects of the main co-existing inorganic species. Moreover, although the intricate mixed effects of the various soil components in real SW effluent, the PHE oxidation efficiency with UVB/PDS is similar to the removal in the synthetic solutions, implying UVB/PDS remains to be the most efficient process for PHE elimination.

4. Conclusion

The results obtained from this study indicate that the UVB based AOPs, e.g., UVB/PDS and UVB/H_2O_2, can eliminate PHE in both simulated and real SW

effluents. The photo-degradation efficiency of PHE is influenced by various parameters including the concentration of oxidants, initial pH and widespread soil inorganic anions (Cl^-, HCO_3^- and NO_3^-). Opposite results are obtained for the effect of Cl^- for UVB assisted H_2O_2 and PDS activation. The presence of Cl^- at alkaline pH inhibits PHE degradation in UVB/H_2O_2, while slightly enhances PHE elimination in the UVB/PDS process at different pH. The experimental results reveal the negligible effect of HCO_3^- in the UVB/PDS system but negative effect in the UVB/H_2O_2 process. Nitrate has negative effect on the PHE degradation in both AOPs. Overall, the UVB/PDS process is much more efficient than UVB/H_2O_2 due to the formation of sulfate radical which is less sensitive to the main inorganic ions present in soil, and could be a promising process to be applied for real SW effluents treatment.

Acknowledgments

Authors gratefully acknowledge the Ministry of Education of China for providing financial support to Yufang TAO for her stay at the Institute of Chemistry of Clermont-Ferrand and Clermont Auvergne University in France. Authors also acknowledge the financial support from the Region Council of Auvergne Rhône Alpes, from the "Féderation des Recherches en Environnement" through the CPER "Environment" founded by the Region Auvergne, the French government and the FEDER (European Community), from PRC program CNRS/NSFC n°270437 and from CAP 20-25 I-site project.

References

Bastviken, D., Sandén, P., Svensson, T., Ståhlberg, C., Magounakis, M., Öberg, G., 2006. Chloride retention and release in a boreal forest soil: effects of soil water residence time and nitrogen and chloride loads. Environmental Science &

Technology 40 (9), 2977-2982.

Beck, S.E., Ryu, H., Boczek, L.A., Cashdollar, J.L., Jeanis, K.M., Rosenblum, J.S., Lawal, O.R., Linden, K.G., 2017. Evaluating UV-C LED disinfection performance and investigating potential dual-wavelength synergy. Water Research 109, 207-216.

Bennedsen, L.R., Muff, J., Sogaard, E.G., 2012. Influence of chloride and carbonates on the reactivity of activated persulfate. Chemosphere 86 (11), 1092-1097.

Bezza, F.A., Chirwa, E.M.N., 2017. The role of lipopeptide biosurfactant on microbial remediation of aged polycyclic aromatic hydrocarbons (PAHs)-contaminated soil. Chemical Engineering Journal 309, 563-576.

Buxton, G.V., Greenstock, C.L., Helman, W.P., Ross, A.B., 1988. Critical review of rate constants for reactions of hydrated electrons, hydrogen atoms and hydroxyl radicals ($\cdot OH/\cdot O^-$) in aqueous solution. Journal of Physical and Chemical Reference Data 17 (2), 513-886.

Cheng, M., Zeng, G., Huang, D., Yang, C., Lai, C., Zhang, C., Liu, Y., 2017. Advantages and challenges of Tween 80 surfactant-enhanced technologies for the remediation of soils contaminated with hydrophobic organic compounds. Chemical Engineering Journal 314, 98-113.

Crabb, N.T., Persinger, H.E., 1964. The determination of polyoxyethylene nonionic surfactants in water at the parts per million level. Journal of the American Oil Chemists' Society 41 (11), 752-755.

Crittenden, J.C., Hu, S., Hand, D.W., Green, S.A., 1999. A kinetic model for H_2O_2/UV process in a completely mixed batch reactor. Water Research 33 (10), 2315-2328.

Deng, J., Shao, Y., Gao, N., Xia, S., Tan, C., Zhou, S., Hu, X., 2013. Degradation of the antiepileptic drug carbamazepine upon different UV-based advanced

oxidation processes in water. Chemical Engineering Journal 222, 150-158.

Du, C., Ma, Z., Zhou, J., Goyne, K.W., 2013. Application of mid-infrared photoacoustic spectroscopy in monitoring carbonate content in soils. Sensors and Actuators, B: Chemical 188, 1167-1175.

Gou, Y., Yang, S., Cheng, Y., Song, Y., Qiao, P., Li, P., Ma, J., 2019. Enhanced anoxic biodegradation of polycyclic aromatic hydrocarbons (PAHs) in aged soil pretreated by hydrogen peroxide. Chemical Engineering Journal 356, 524-533.

Grigor'ev, A., Makarov, I., Pikaev, A., 1987. Formation of Cl_2^- in the bulk of solution during radiolysis of concentrated aqueous solutions of chlorides. Khimiya Vysokikh Ehnergij 21 (2), 123-126.

Hasegawa, K., Neta, P., 1978. Rate constants and mechanisms of reaction of chloride (Cl_2^-) radicals. The Journal of Physical Chemistry 82 (8), 854-857.

Herrmann, H., 2007. On the photolysis of simple anions and neutral molecules as sources of O^-/OH, SO_x^- and Cl in aqueous solution. Physical Chemistry Chemical Physics 9 (30), 3935-3964.

Herrmann, H., Reese, A., Zellner, R., 1995. Time-resolved UV/Vis diode array absorption spectroscopy of SO_x^-(x= 3, 4, 5) radical anions in aqueous solution. Journal of Molecular Structure 348, 183-186.

Huang, W., Bianco, A., Brigante, M., Mailhot, G., 2018. UVA-UVB activation of hydrogen peroxide and persulfate for advanced oxidation processes: efficiency, mechanism and effect of various water constituents. Journal of Hazardous Materials 347, 279-287.

Jayson, G., Parsons, B., Swallow, A.J., 1973. Some simple, highly reactive, inorganic chlorine derivatives in aqueous solution. their formation using pulses of radiation and their role in the mechanism of the fricke dosimeter. Journal of The Chemical

Society, Faraday Transactions 1: Physical Chemistry in Condensed Phases 69, 1597-1607.

Joseph, C.G., Taufiq-Yap, Y.H., Li Puma, G., Sanmugam, K., Quek, K.S., 2016. Photocatalytic degradation of cationic dye simulated wastewater using four radiation sources, UVA, UVB, UVC and solar lamp of identical power output. Desalination and Water Treatment 57 (17), 7976-7987.

Keen, O.S., Love, N.G., Linden, K.G., 2012. The role of effluent nitrate in trace organic chemical oxidation during UV disinfection. Water Research 46 (16), 5224-5234.

Kläning, U.K., Wolff, T., 1985. Laser flash photolysis of HClO, ClO^-, HBrO, and BrO^- in aqueous solution. reactions of Cl^- and Br^- atoms. Berichte der Bunsengesellschaft für Physikalische Chemie 89 (3), 243-245.

Kuhlman, M., Greenfield, T., 1999. Simplified soil washing processes for a variety of soils. Journal of Hazardous Materials 66 (1-2), 31-45.

Lamichhane, S., Bal Krishna, K.C., Sarukkalige, R., 2017. Surfactant-enhanced remediation of polycyclic aromatic hydrocarbons: A review. Journal of Environmental Management 199, 46-61.

Li, Y., Liao, X., Huling, S.G., Xue, T., Liu, Q., Cao, H., Lin, Q., 2019. The combined effects of surfactant solubilization and chemical oxidation on the removal of polycyclic aromatic hydrocarbon from soil. Science of The Total Environment 647, 1106-1112.

Liu, Y., He, X., Duan, X., Fu, Y., Fatta-Kassinos, D., Dionysiou, D.D., 2016. Significant role of UV and carbonate radical on the degradation of oxytetracycline in UV-AOPs: kinetics and mechanism. Water Research 95, 195-204.

Lu, J., Bai, Z., Velthof, G.L., Wu, Z., Chadwick, D., Ma, L., 2019. Accumulation and leaching of nitrate in soils in wheat-maize production in China. Agricultural Water Management 212, 407-415.

Lyon, B.A., Dotson, A.D., Linden, K.G., Weinberg, H.S., 2012. The effect of inorganic precursors on disinfection byproduct formation during UV-chlorine/chloramine drinking water treatment. Water Research 46 (15), 4653-4664.

Mack, J., Bolton, J.R., 1999. Photochemistry of nitrite and nitrate in aqueous solution: a review. Journal of Photochemistry and Photobiology A 128 (1), 1-13.

Manoli, E., Samara, C., 1999. Polycyclic aromatic hydrocarbons in natural waters: sources, occurrence and analysis. Trends in Analytical Chemistry 18 (6), 417-428.

Marion, A., Brigante, M., Mailhot, G., 2018. A new source of ammonia and carboxylic acids in cloud water: The first evidence of photochemical process involving an iron-amino acid complex. Atmospheric Environment 195, 179-186.

Mark, G., Schuchmann, M.N., Schuchmann, H., von Sonntag, C., 1990. The photolysis of potassium peroxodisulphate in aqueous solution in the presence of tert-butanol: a simple actinometer for 254 nm radiation. Journal of Photochemistry and Photobiology A 55 (2), 157-168.

Minella, M., Bertinetti, S., Hanna, K., Minero, C., Vione, D., 2019. Degradation of ibuprofen and phenol with a Fenton-like process triggered by zero-valent iron (ZVI-Fenton). Environmental Research 179, 108750.

Mosteo, R., Varon-Lopez, A., Muzard, D., Benitez, N., Giannakis, S., Pulgarin, C., 2020. Visible light plays a significant role during bacterial inactivation by the photo-Fenton process, even at sub-critical light intensities. Water Research,

115636.

Mousset, E., Oturan, N., Hullebusch, E.D.V., Guibaud, G., Esposito, G., Oturan, M.A., 2014. Influence of solubilizing agents (cyclodextrin or surfactant) on phenanthrene degradation by electro-Fenton process – study of soil washing recycling possibilities and environmental impact. Water Research 48 (1), 306-316.

Neta, P., Huie, R.E., Ross, A.B., 1988. Rate constants for reactions of inorganic radicals in aqueous solution. Journal of Physical and Chemical Reference Data 17 (3), 1027-1284.

Olmez-Hanci, T., Arslan-Alaton, I., 2013. Comparison of sulfate and hydroxyl radical based advanced oxidation of phenol. Chemical Engineering Journal 224, 10-16.

Ortega, L.M., Lebrun, R., Blais, J., Hausler, R., Drogui, P., 2008. Effectiveness of soil washing, nanofiltration and electrochemical treatment for the recovery of metal ions coming from a contaminated soil. Water Research 42 (8-9), 1943-1952.

Petrová, Š., Rezek, J., Soudek, P., Vaněk, T., 2017. Preliminary study of phytoremediation of brownfield soil contaminated by PAHs. Science of The Total Environment 599, 572-580.

Reddy, K.R., Ala, P.R., Sharma, S., Kumar, S.N., 2006. Enhanced electrokinetic remediation of contaminated manufactured gas plant soil. Engineering Geology 85 (1-2), 132-146.

Shin, K.-H., Kim, K.-W., Ahn, Y., 2006. Use of biosurfactant to remediate phenanthrene-contaminated soil by the combined solubilization–biodegradation process. Journal of Hazardous Materials 137 (3), 1831-1837.

Sörensen, M., Frimmel, F.H., 1997. Photochemical degradation of hydrophilic xenobiotics in the UVH_2O_2 process: Influence of nitrate on the degradation rate

of EDTA, 2-amino-1-naphthalenesulfonate, diphenyl-4-sulfonate and 4, 4′-diaminostilbene-2, 2′-disulfonate. Water Research 31 (11), 2885-2891.

Tan, C., Gao, N., Deng, Y., Zhang, Y., Sui, M., Deng, J., Zhou, S., 2013. Degradation of antipyrine by UV, UV/H_2O_2 and UV/PS. Journal of Hazardous Materials 260, 1008-1016.

Tao, Y., Brigante, M., Zhang, H., Mailhot, G., 2019. Phenanthrene degradation using Fe (III)-EDDS photoactivation under simulated solar light: A model for soil washing effluent treatment. Chemosphere 236, 124366.

Trellu, C., Ganzenko, O., Papirio, S., Pechaud, Y., Oturan, N., Huguenot, D., Van Hullebusch, E.D., Esposito, G., Oturan, M.A., 2016. Combination of anodic oxidation and biological treatment for the removal of phenanthrene and Tween 80 from soil washing solution. Chemical Engineering Journal 306, 588-596.

Trellu, C., Oturan, N., Pechaud, Y., van Hullebusch, E.D., Esposito, G., Oturan, M.A., 2017. Anodic oxidation of surfactants and organic compounds entrapped in micelles - Selective degradation mechanisms and soil washing solution reuse. Water Research 118, 1.

Wan, D., Zuo, J., Chen, Y., Chen, Q., Zuo, Y., 2018. Photodegradation of amitriptyline in Fe(III)-citrate-oxalate binary system: Synergistic effect and mechanism. Chemosphere 210, 224-231.

Wang, C., Shu, L., Zhou, S., Yu, H., Zhu, P., 2019. Effects of alternate partial root-zone irrigation on the utilization and movement of nitrates in soil by tomato plants. Scientia Horticulturae 243, 41-47.

Wu, Y., Bianco, A., Brigante, M., Dong, W., de Sainte-Claire, P., Hanna, K., Mailhot, G., 2015. Sulfate radical photogeneration using Fe-EDDS: influence of critical parameters and naturally occurring scavengers. Environmental Science &

Technology 49 (24), 14343-14349.

Xiao, Y., Zhang, L., Zhang, W., Lim, K., Webster, R.D., Lim, T., 2016. Comparative evaluation of iodoacids removal by UV/persulfate and UV/H_2O_2 processes. Water Research 102, 629-639.

Xu, Y., Lin, Z., Zhang, H., 2016. Mineralization of sucralose by UV-based advanced oxidation processes: UV/PDS versus UV/H_2O_2. Chemical Engineering Journal 285, 392-401.

Yang, K., Zhu, L., Xing, B., 2006. Enhanced soil washing of phenanthrene by mixed solutions of TX100 and SDBS. Environmental Science & Technology 40 (13), 4274-4280.

Yang, S., Wang, P., Yang, X., Shan, L., Zhang, W., Shao, X., Niu, R., 2010. Degradation efficiencies of azo dye acid orange 7 by the interaction of heat, UV and anions with common oxidants: persulfate, peroxymonosulfate and hydrogen peroxide. Journal of Hazardous Materials 179 (1-3), 552-558.

Yang, Y., Pignatello, J.J., Ma, J., Mitch, W.A., 2014. Comparison of halide impacts on the efficiency of contaminant degradation by sulfate and hydroxyl radical-based advanced oxidation processes (AOPs). Environmental Science & Technology 48 (4), 2344-2351.

Yang, Y., Pignatello, J.J., Ma, J., Mitch, W.A., 2016. Effect of matrix components on UV/H_2O_2 and UV/$S_2O_8^{2-}$ advanced oxidation processes for trace organic degradation in reverse osmosis brines from municipal wastewater reuse facilities. Water Research 89, 192-200.

Yeom, I.T., Ghosh, M.M., Cox, C.D., Robinson, K.G., 1995. Micellar solubilization of polynuclear aromatic hydrocarbons in coal tar-contaminated soils. Environmental Science & Technology 29 (12), 3015-3021.

566 Yu, X.-Y., Barker, J.R., 2003. Hydrogen peroxide photolysis in acidic aqueous
567 solutions containing chloride ions. II. Quantum yield of HO•(Aq) radicals.
568 Journal of Physical Chemistry A 107 (9), 1325-1332.
569 Zellner, R., Exner, M., Herrmann, H., 1990. Absolute OH quantum yields in the laser
570 photolysis of nitrate, nitrite and dissolved H_2O_2 at 308 and 351 nm in the
571 temperature range 278–353 K. Journal of Atmospheric Chemistry 10 (4),
572 411-425.
573 Zhang, R., Sun, P., Boyer, T.H., Zhao, L., Huang, C.-H., 2015. Degradation of
574 pharmaceuticals and metabolite in synthetic human urine by UV, UV/H_2O_2, and
575 UV/PDS. Environmental Science & Technology 49 (5), 3056-3066.
576 Zhou, L., Ferronato, C., Chovelon, J., Sleiman, M., Richard, C., 2017a. Investigations
577 of diatrizoate degradation by photo-activated persulfate. Chemical Engineering
578 Journal 311, 28-36.
579 Zhou, L., Sleiman, M., Ferronato, C., Chovelon, J., Sainte-claire, P.D., Richard, C.,
580 2017b. Sulfate radical induced degradation of β2-adrenoceptor agonists
581 salbutamol and terbutaline: Phenoxyl radical dependent mechanisms. Water
582 research 123, 715-723.
583 Zuo, Z., Cai, Z., Katsumura, Y., Chitose, N., Muroya, Y., 1999. Reinvestigation of the
584 acid–base equilibrium of the (bi) carbonate radical and pH dependence of its
585 reactivity with inorganic reactants. Radiation Physics and Chemistry 55 (1),
586 15-23.
587

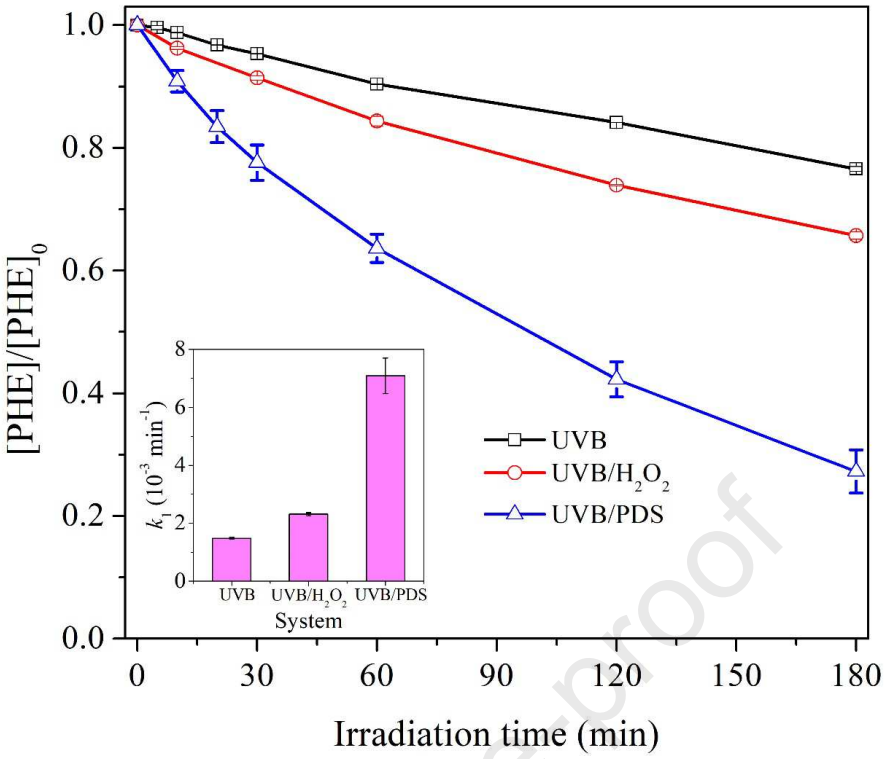

Figure 1. Degradation of PHE in the presence of TW80 in different systems. Inserts are the corresponding pseudo-first order rate constants. Initial conditions are [PHE] = 10 mg L^{-1}, [TW80] = 0.5 g L^{-1}, [PDS] = [H_2O_2] = 5 mM, pH 3.3 ± 0.1.

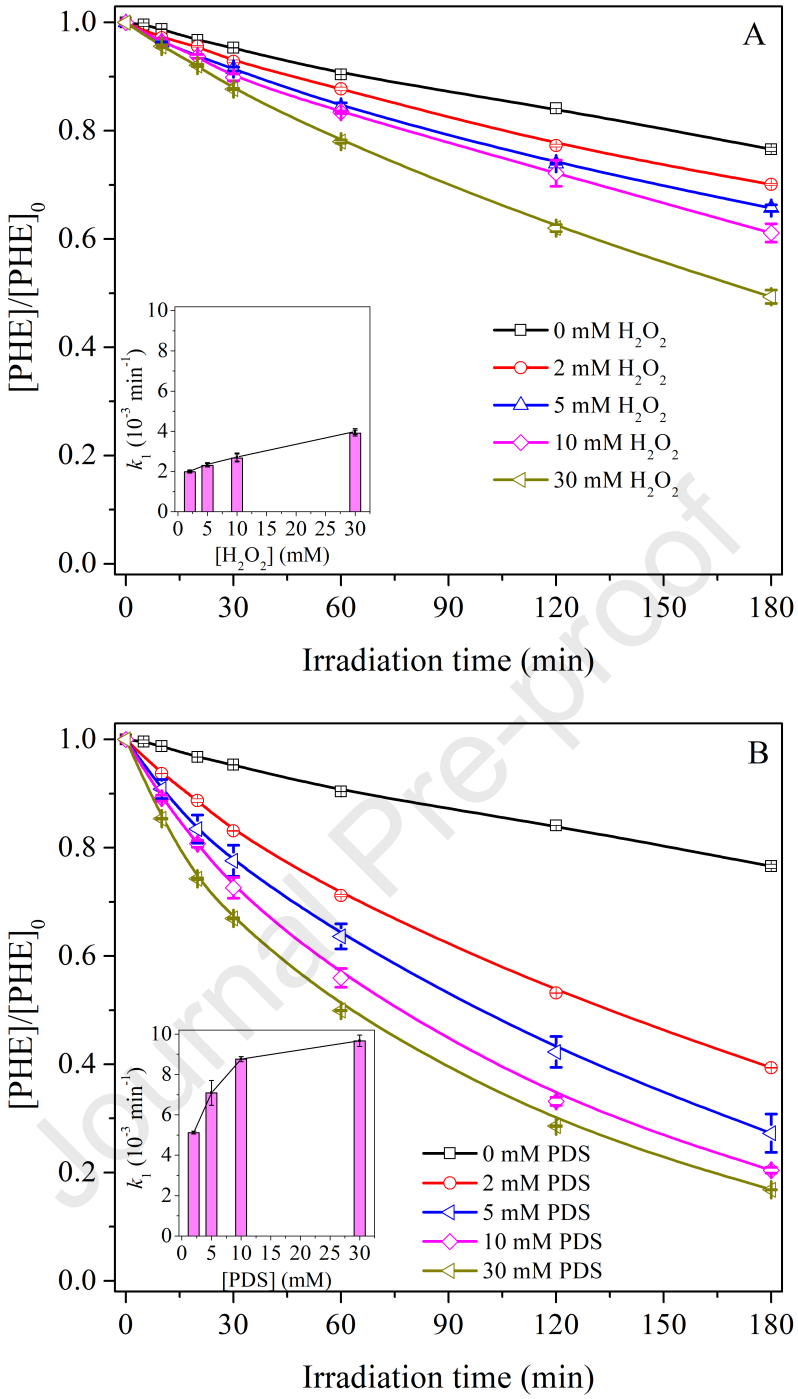

Figure 2. Influence of oxidant concentration on the photo-degradation of PHE. Inserts are the corresponding pseudo first order rate constants. A) UVB/H_2O_2; B) UVB/PDS. Initial conditions are [PHE] = 10 mg L^{-1}, [TW80] = 0.5 g L^{-1}, pH 3.3 ± 0.1.

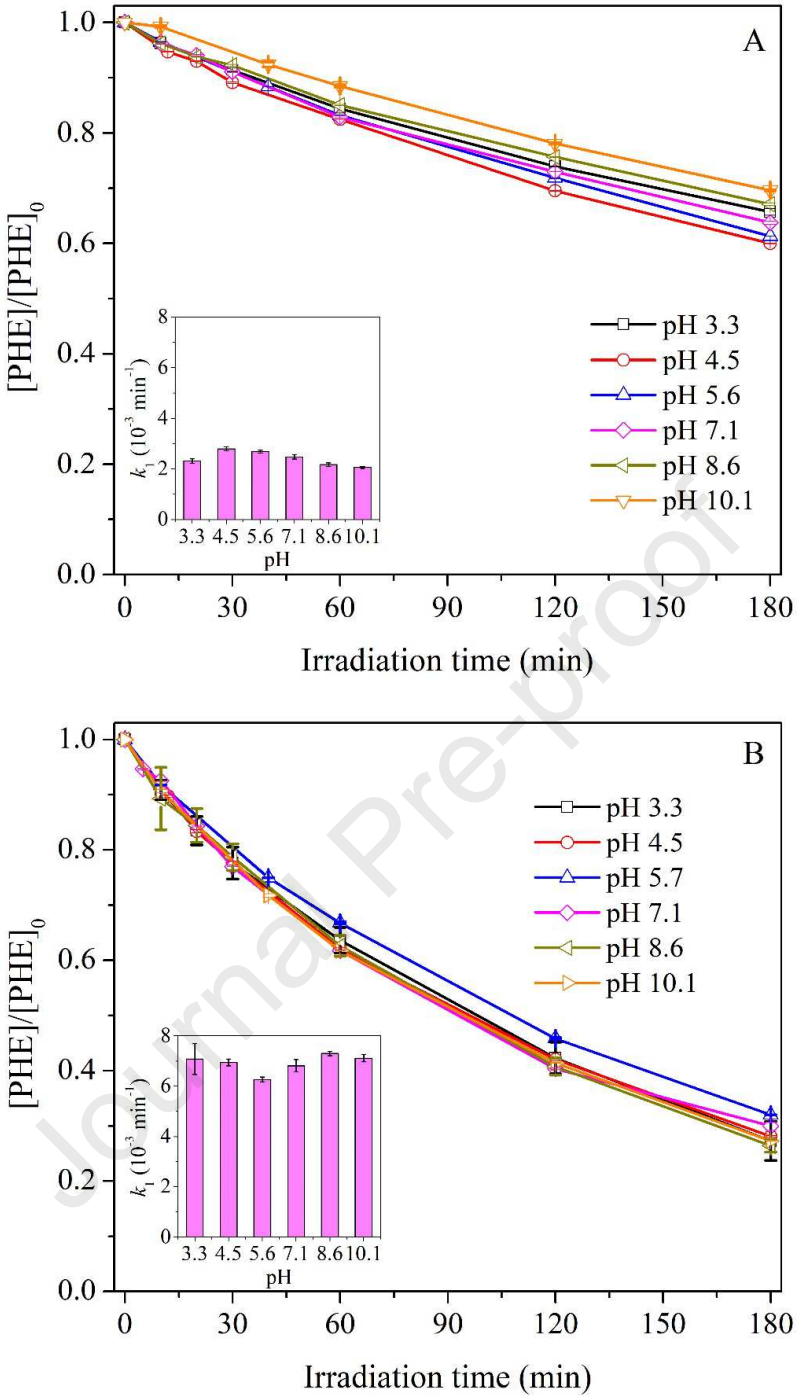

Figure 3. Influence of initial solution pH on the photo-degradation of PHE. Inserts are the corresponding pseudo first order rate constants. A) UVB/H_2O_2; B) UVB/PDS. Initial conditions are: [PHE] = 10 mg L^{-1}, [TW80] = 0.5 g L^{-1}, [PDS] = [H_2O_2] = 5 mM.

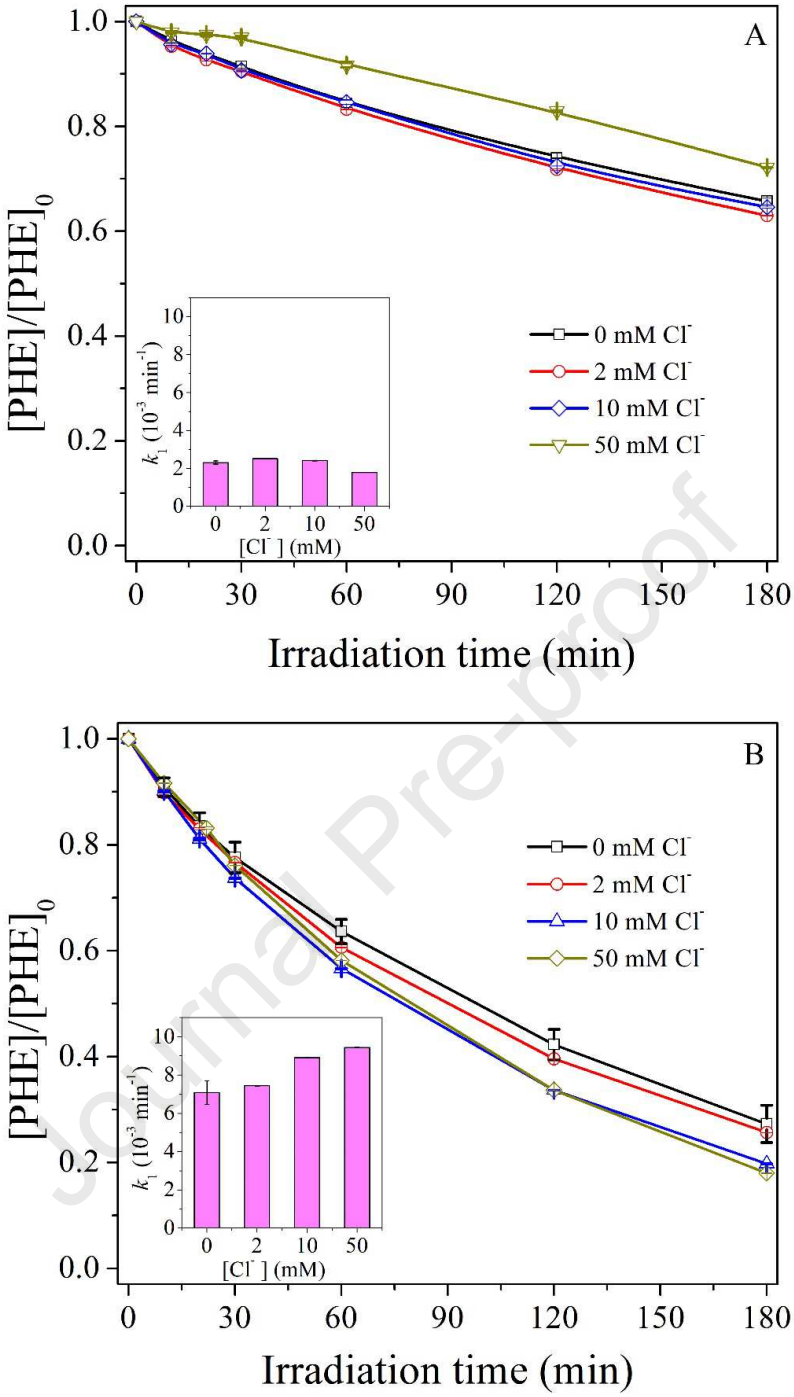

Figure 4. Influence of Cl^- concentration on the photo-degradation of PHE. A) UVB/H_2O_2; B) UVB/PDS. Insets are the corresponding first-order rate constants. Initial conditions are: [PHE] = 10 mg L^{-1}, [TW80] = 0.5 g L^{-1}, [PDS] = [H_2O_2] = 5 mM, pH 3.3 ± 0.1.

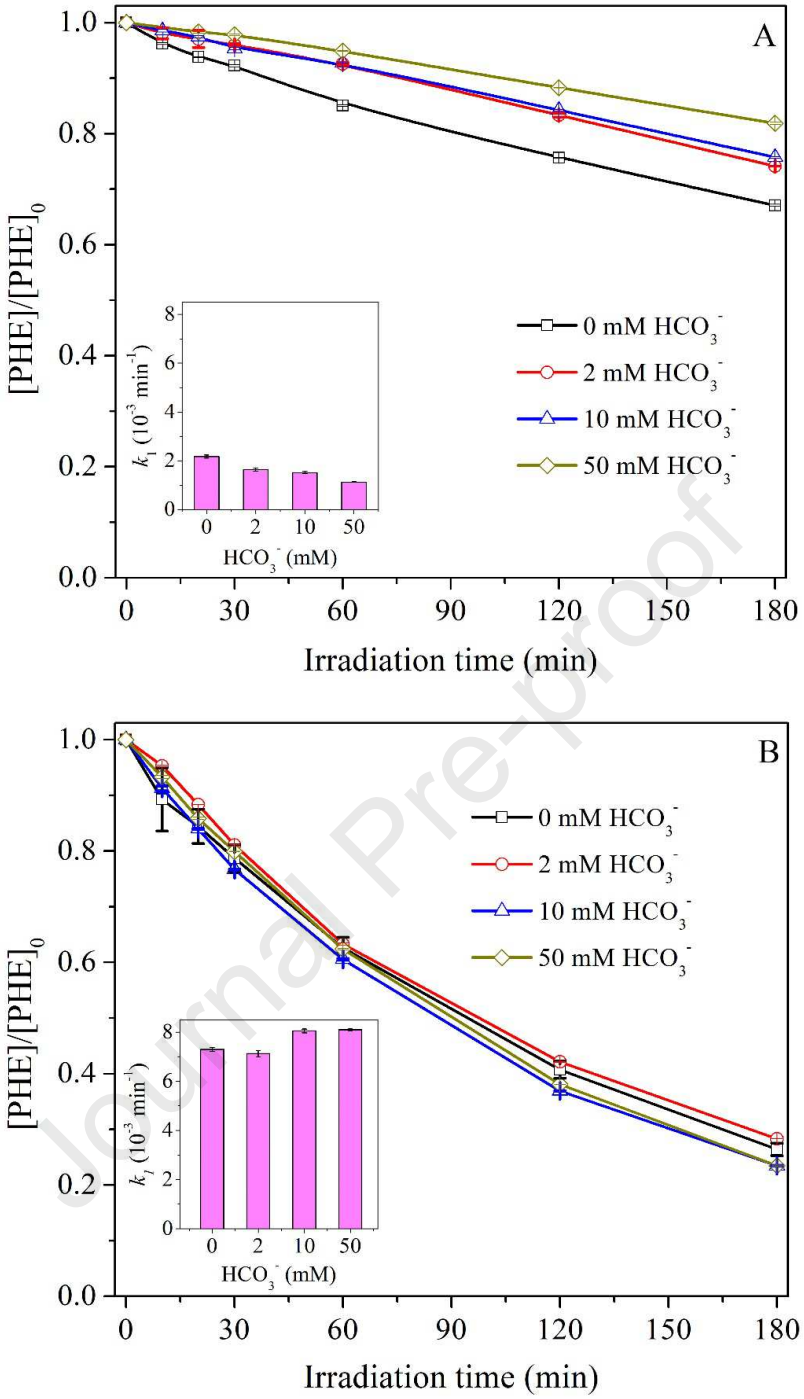

Figure 5. Influence of HCO_3^- concentration on the photo-degradation of PHE. A) UVB/H_2O_2; B) UVB/PDS. Insets are the corresponding first-order rate constants. Initial conditions are: [PHE] = 10 mg L^{-1}, [TW80] = 0.5 g L^{-1}, [PDS] = [H_2O_2] = 5 mM, pH 8.6 ± 0.1.

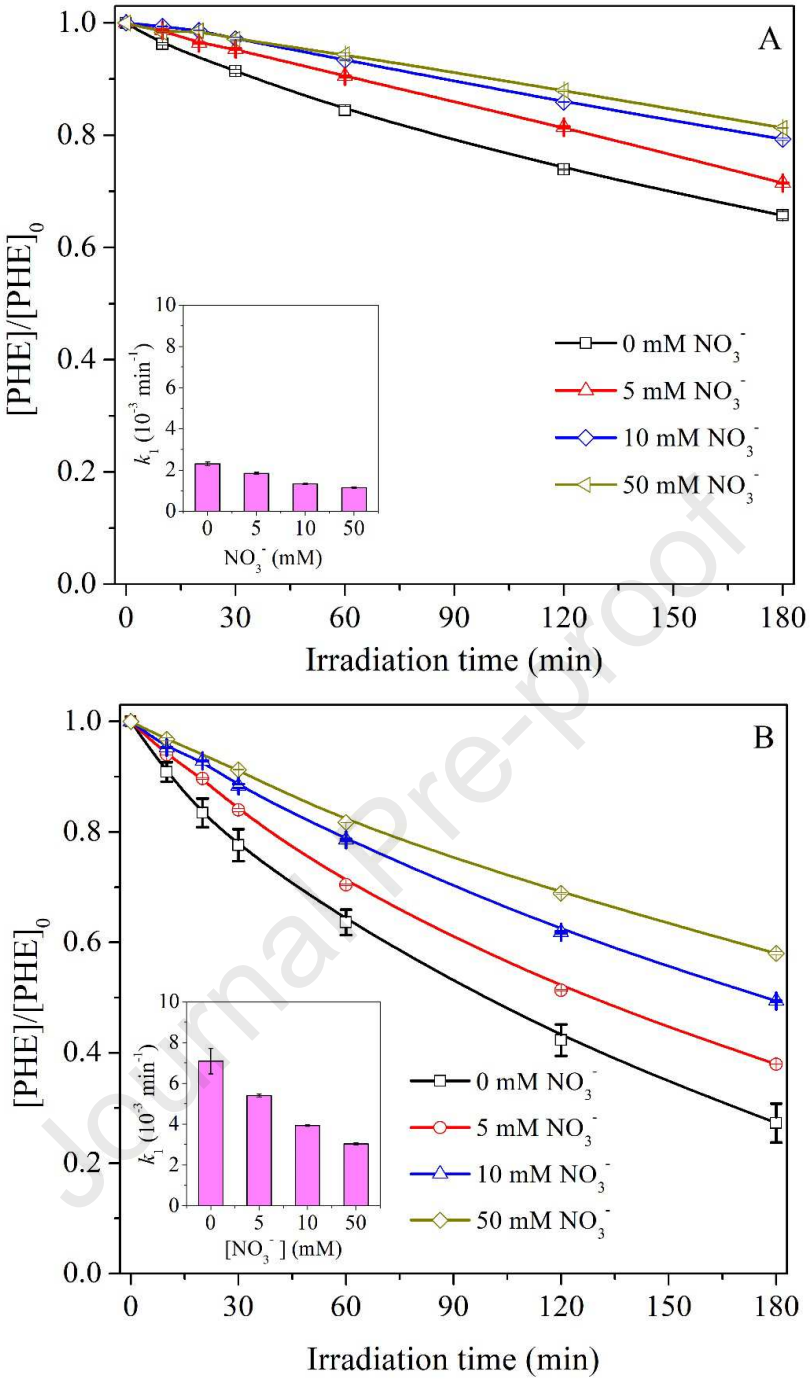

Figure 6. Influence of NO_3^- concentration on the photo-degradation of PHE. A) UVB/H_2O_2; B) UVB/PDS. Insets are the corresponding first-order rate constants. Initial conditions are: [PHE] = 10 mg L^{-1}, [TW80] = 0.5 g L^{-1}, [PDS] = [H_2O_2] = 5 mM, pH 3.3 ± 0.1.

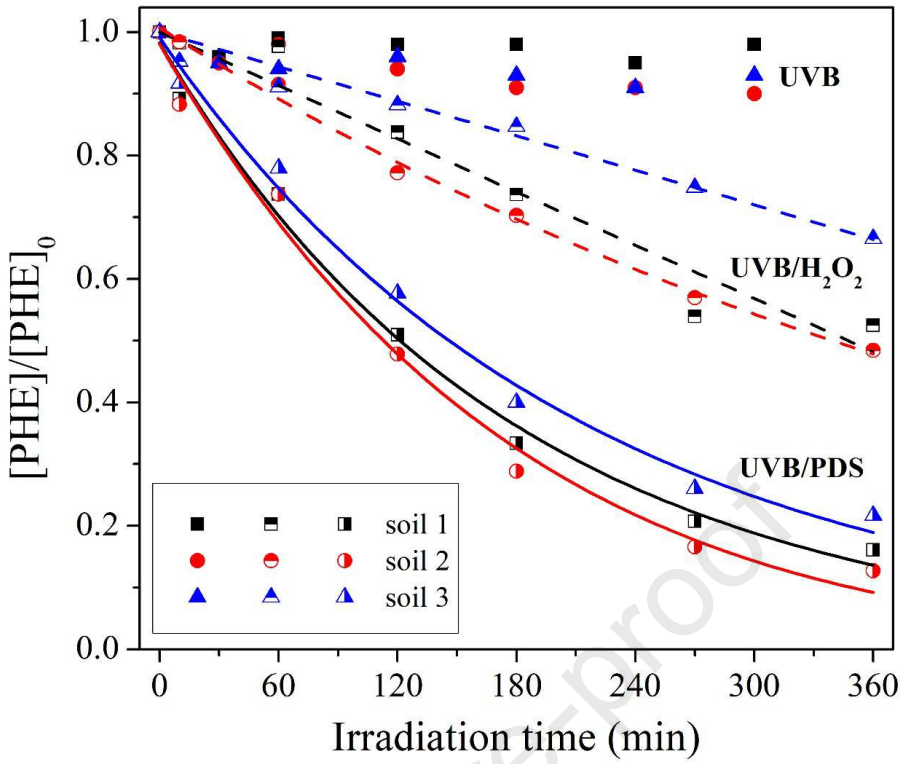

Figure 7. Degradation of PHE with three real SW effluents in different systems. Initial conditions are [PDS] = [H_2O_2] = 5 mM.

Highlights

- PDS is more efficient than H_2O_2 for UVB decay of PHE in soil washing (SW) effluent
- UVB/PDS process is less impacted by the inorganic ions (Cl^-, HCO_3^- and NO_3^-)
- UVB/PDS is a promising and sustainable process for real SW effluent treatment

Figure captions

Figure 1. Degradation of PHE in the presence of TW80 in different systems. Inserts are the corresponding pseudo-first order rate constants. Initial conditions are [PHE] = 10 mg L^{-1}, [TW80] = 0.5 g L^{-1}, [PDS] = [H_2O_2] = 5 mM, pH 3.3 ± 0.1.

Figure 2. Influence of oxidant concentration on the photo-degradation of PHE. Inserts are the corresponding pseudo first order rate constants. A) UVB/H_2O_2; B) UVB/PDS. Initial conditions are [PHE] = 10 mg L^{-1}, [TW80] = 0.5 g L^{-1}, pH 3.3 ± 0.1.

Figure 3. Influence of initial solution pH on the photo-degradation of PHE. Inserts are the corresponding pseudo first order rate constants. A) UVB/H_2O_2; B) UVB/PDS. Initial conditions are: [PHE] = 10 mg L^{-1}, [TW80] = 0.5 g L^{-1}, [PDS] = [H_2O_2] = 5 mM.

Figure 4. Influence of Cl^- concentration on the photo-degradation of PHE. A) UVB/H_2O_2; B) UVB/PDS. Insets are the corresponding first-order rate constants. Initial conditions are: [PHE] = 10 mg L^{-1}, [TW80] = 0.5 g L^{-1}, [PDS] = [H_2O_2] = 5 mM, pH 3.3 ± 0.1.

Figure 5. Influence of HCO_3^- concentration on the photo-degradation of PHE. A) UVB/H_2O_2; B) UVB/PDS. Insets are the corresponding first-order rate constants. Initial conditions are: [PHE] = 10 mg L^{-1}, [TW80] = 0.5 g L^{-1}, [PDS] = [H_2O_2] = 5 mM, pH 8.6 ± 0.1.

Figure 6. Influence of NO_3^- concentration on the photo-degradation of PHE. A) UVB/H_2O_2; B) UVB/PDS. Insets are the corresponding first-order rate constants. Initial conditions are: [PHE] = 10 mg L^{-1}, [TW80] = 0.5 g L^{-1}, [PDS] = [H_2O_2] = 5 mM, pH 3.3 ± 0.1.

Figure 7. Degradation of PHE with three real SW effluents in different systems. Initial conditions are [PDS] = [H_2O_2] = 5 mM.